δ-EF1 is a negative regulator of *Ihh* in the developing growth plate

Ellen Bellon, Frank P. Luyten, and Przemko Tylzanowski

Laboratory of Skeletal Development and Joint Disorders, Division of Rheumatology, Department of Musculoskeletal Sciences, University of Leuven, Leuven 3000, Belgium

Indian hedgehog (*Ihh*) regulates proliferation and differentiation of chondrocytes in the growth plate. Although the biology of *Ihh* is currently well documented, its transcriptional regulation is poorly understood. δ-EF1 is a two-handed zinc finger/homeodomain transcriptional repressor. Targeted inactivation of mouse *δ-EF1* leads to skeletal abnormalities including disorganized growth plates, shortening of long bones, and joint fusions, which are reminiscent of defects associated with deregulation of *Ihh* signaling. Here, we show that the absence of *δ-EF1* results in delayed hypertrophic differentiation of chondrocytes and increased cell proliferation in the growth plate. Further, we demonstrate that δ-EF1 binds to the putative regulatory elements in intron 1 of *Ihh* in vitro and in vivo, resulting in down-regulation of *Ihh* expression. Finally, we show that *δ-EF1* haploinsufficiency leads to a postnatal increase in trabecular bone mass associated with enhanced *Ihh* expression. In summary, we have identified δ-EF1 as an in vivo negative regulator of *Ihh* expression in the growth plate.

Introduction

Endochondral ossification is a multistep process in which prechondrogenic mesenchymal cells condensate and form distinct cartilaginous elements. Subsequently, this cartilaginous template forms a growth plate necessary for longitudinal growth. During development, the growth plate stratifies into zones of resting, proliferating, prehypertrophic, and hypertrophic chondrocytes, forming a highly interactive structure where each zone is influenced by events in the flanking zones and the perichondrium (Kronenberg, 2003).

Initiation of chondrogenesis begins with induction of the transcription factor Sox9 in limb mesenchyme and subsequent condensation of mesenchymal cells (Bi et al., 1999). Next, the condensed cells differentiate into chondrocytes that, among others, express transcription factors Sox5 and -6 (Smits et al., 2004) as well as matrix protein collagen type II. As the chondroblasts mature, they flatten and align in organized columnar structures along the longitudinal axis of the cartilage template, forming a transient pool of prehypertrophic cells. Finally, these cells exit the cell cycle, enlarge in size, and undergo hypertrophy. At this stage, cells in the perichondrium differentiate into osteoblasts that deposit an extracellular matrix, which will mineralize to form the bone collar. Hypertrophic chondrocytes express collagen type X and produce VEGF that stimulates blood vessel invasion in the calcified cartilage (Provot and Schipani, 2005). Invading osteoclasts will resorb the cartilage matrix, and osteoblasts will deposit bone matrix on the cartilage remnants (Kronenberg, 2003; Provot and Schipani, 2005).

Several factors regulate the process of endochondral bone formation, and one of the more prominent ones is a member of the conserved hedgehog (Hh) family of secreted proteins, Indian hedgehog (IHH; Bitgood and McMahon, 1995; Vortkamp et al., 1996; Hammerschmidt et al., 1997). Hh proteins transduce their signal by binding to a 12-pass transmembrane receptor protein Patched (Ptc). In the absence of Hh, Ptc represses the activation of another multipass transmembrane protein, smoothened (smo; Chen and Struhl, 1996; Marigo et al., 1996; Stone et al., 1996). Binding of Hh ligands to Ptc relieves the repression of smo, activating the Hh signal transduction pathway that is mediated by Gli transcription factors (Gli1, Gli2, and Gli3). Although Gli1 functions as an activator, Gli2 and -3 can act either as transcriptional activators or repressors depending on the cellular context (Matise and Joyner, 1999; Mullor et al., 2002; Cohen, 2003; Nieuwenhuis and Hui, 2005).

Correspondence to Przemko Tylzanowski: przemko@med.kuleuven.be

Abbreviations used in this paper: ChIP, chromatin immunoprecipitation; dpc, days postcoitum; DEXA, dual energy x-ray absorptiometry; EMSA, electrophoretic mobility shift assay; Hh, hedgehog; HH, Hamburger-Hamilton; HZ, heterozygous; Ihh, Indian hedgehog; KO, knockout; PPR, PTHrP receptor; pQCT, peripheral quantitative computed tomography; Ptc, patched; PTHrP, parathyroid hormone–related protein; smo, smoothened; WT, wild type.

© 2009 Bellon et al. This article is distributed under the terms of an Attribution–Noncommercial–Share Alike–No Mirror Sites license for the first six months after the publication date (see http://www.jcb.org/misc/terms.shtml). After six months it is available under a Creative Commons License (Attribution–Noncommercial–Share Alike 3.0 Unported license, as described at http://creativecommons.org/licenses/by-nc-sa/3.0/).

The Rockefeller University Press $30.00
J. Cell Biol. Vol. 187 No. 5 685–699
www.jcb.org/cgi/doi/10.1083/jcb.200904034

Ihh is expressed in prehypertrophic and hypertrophic chondrocytes controlling several important differentiation steps in the development of the endochondral skeleton. *Ihh* regulates chondrocyte differentiation by activating the expression of parathyroid hormone–related protein (PTHrP; Pthlh) in the periarticular cells. PTHrP is a paracrine signaling molecule that diffuses toward the prehypertrophic zone and signals through its receptor, PTHrP receptor (PPR), to inhibit hypertrophic differentiation, ensuring a supply of proliferating chondrocytes essential for the formation of hypertrophic cells and thus longitudinal growth (Vortkamp et al., 1996; Lanske et al., 1999; Karp et al., 2000). *Ihh* also regulates chondrocyte proliferation independently of PTHrP. Analysis of *Ihh*-null mice expressing a constitutively active mutant of PPR showed that the proliferation defect in *Ihh*-null mice was independent of PTHrP signaling (St Jacques et al., 1999; Karp et al., 2000; Long et al., 2001). Furthermore, *Ihh* also regulates ossification of the perichondrium, where it is required for the initial specification of osteoblast progenitor cells but not for the formation of mature osteoblasts (Rodda and McMahon, 2006). Besides its function in osteo- and chondrogenic differentiation, *Ihh* is also involved in the endothelial cell fate determination and blood vessel formation because $Ihh^{-/-}$ blood vessels do invade the mutant hypertrophic cartilage but cannot persist (Colnot et al., 2005).

Even though *Ihh* is one of the key regulators of endochondral ossification, surprisingly little is known about the mechanisms by which the expression of *Ihh* is regulated. It has been reported that one of the key transcriptional regulators of endochondral bone formation, Runx2, is activating the *Ihh* promoter in vitro (Yoshida et al., 2004). *Ihh* expression could also be a target of Wnt signaling because a direct interaction between the *Ihh* promoter and the β-catenin–Lef1 complex in vivo has been demonstrated (Später et al., 2006).

A precise regulation of *Ihh* is important for endochondral bone formation, as shown by various skeletal phenotypes induced by modulation of *Ihh* gene expression. For example, *Ihh*-null mice exhibit short-limb dwarfism with reduced chondrocyte proliferation and extensive hypertrophy (St-Jacques et al., 1999). *Ihh* overexpression, however, leads to delayed chondrocyte differentiation, delayed ossification of the long bones, and expansion of the growth plate with increased proliferation (Vortkamp et al., 1996; Kobayashi et al., 2005). Additionally, misexpression of Hh proteins in the cartilage leads to joint fusions (Tavella et al., 2004).

Interestingly, the described phenotypes of *Ihh* overexpression are very similar to skeletal abnormalities observed in *δ-EF1*–null mice (Takagi et al., 1998). Targeted inactivation of the *δ-EF1* gene leads to craniofacial abnormalities, sternum, rib, and limb defects such as shortening and broadening of long bones, and joint and carpal/tarsal bone fusions (Takagi et al., 1998).

δ-EF1 is a two-handed zinc finger transcription factor (Funahashi et al., 1993). The gene has been described independently as Zfxh1a in mice, ZEB/AREB6/Nil-2-a in humans, BZP in hamsters, and Zfhep in rats (Williams et al., 1991; Watanabe et al., 1993; Franklin et al., 1994; Genetta et al., 1994; Sekido et al., 1996; Cabanillas and Darling, 1996). δ-EF1 binds DNA as a monomer to bipartite CACCT(G) sequences separated by 8–60 nucleotides and located near (±2 kb) the promoter start site. δ-EF1 has been proposed to be a transcriptional repressor–binding E2 box containing sequences and negatively regulating muscle differentiation in vitro (Postigo and Dean, 1997), integrin expression in myoblasts (Jethanandani and Kramer, 2005), and vascular smooth muscle cell differentiation (Nishimura et al., 2006). Additionally, the repressor function of δ-EF1 in vitro has been shown for *Col2a1* promoter activity in chondrocytes and for *Pro-α1-collagen* gene expression in osteoblasts (Murray et al., 2000; Terraz et al., 2001). *δ-EF1* is expressed in the lens, the central nervous system, skeletal precursors, the notochord, the myotome, and the limb bud mesenchyme (Takagi et al., 1998; Tylzanowski et al., 2003). Postnatally, δ-EF1 protein expression was detected in the growth plate and articular and meniscal cartilage of mature mice (Davies et al., 2002).

In the present study, we identified *δ-EF1* as a candidate regulator gene of *Ihh* expression in the growth plate of mice. We show that δ-EF1 binds to the *Ihh* intron 1 transcription regulatory element in vitro and in vivo and that absence of *δ-EF1* leads to temporal deregulation of *Ihh* in developing limbs. Finally we demonstrate that haploinsufficiency for *δ-EF1* associated with enhanced *Ihh* expression leads to increased bone mass in adult mice.

Results

δ-EF1–null mice exhibit defects in hypertrophic differentiation

Detailed description of the developing bones of $\delta\text{-}EF1^{-/-}$ mice has not been published to date. To better understand the observed skeletal phenotype, we performed histological analysis of limbs from *δ-EF1*–null mice at different stages of development.

At 12.5 days postcoitum (dpc), no significant differences were detected between mutant and wild-type (WT) limbs (unpublished data). The first signs of calcification in the WT humerus were visible at 13.5 dpc with the formation of a bone collar, whereas in $\delta\text{-}EF1^{-/-}$ mice, this process was delayed (unpublished data). At 14.5 dpc, limbs of $\delta\text{-}EF1^{-/-}$ mice were shorter than limbs of WT mice (Fig. 1, A and B). Histological analysis revealed that the length of the hypertrophic zone was reduced in $\delta\text{-}EF1^{-/-}$ mice as compared with WT mice (Fig. 1, C and D, compare red and black bars; and Fig. 1, I, J, and K, which shows the quantification of the different cartilage zones), whereas the zones of resting and proliferating chondrocytes were enlarged (Fig. 1, E, F, and K), but there was no apparent difference in columnar organization (Fig. 1, G and H). At 16.5 dpc, the delay in hypertrophic differentiation became more pronounced (Fig. 1, A′–K′) and, in addition, we observed defects in columnar cell organization with fewer stacks of cells (Fig. 1, G′ and H′, arrowheads). This phenotype became more pronounced at 18.5 dpc, where a population of enlarged, oval chondrocytes was present instead of stacks of flat-shaped chondrocytes (Fig. 1, G′′ and H′′, arrowheads).

Chondrocyte hypertrophy was further analyzed by in situ hybridization with probes for *Col2a1* and *Col10a1* mRNA

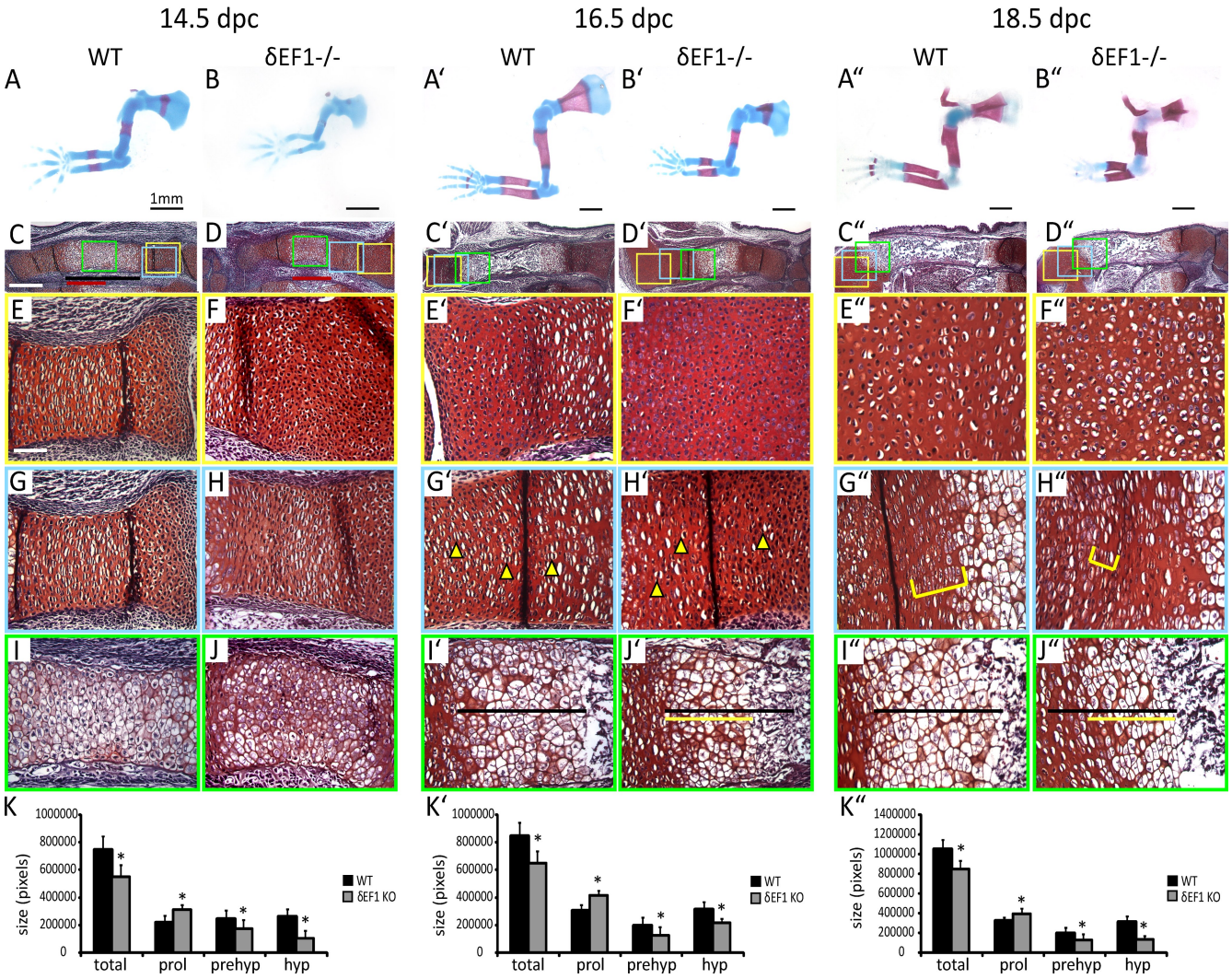

Figure 1. **Analysis of the skeletogenesis in δ-EF1$^{-/-}$ mice.** (A–B′′) Alizarin red/Alcian blue staining of forelimbs of WT and *δ-EF1*$^{-/-}$ mice at 14.5 dpc (A and B), 16.5 dpc (A′ and B′), and 18.5 dpc (A′′ and B′′). (C–D′′) Safranin O staining of humerus of WT and *δ-EF1*$^{-/-}$ mice at 14.5 dpc (C and D), 16.5 dpc (C′ and D′), and 18.5 dpc (C′′–D′′). The yellow, blue, and green rectangles correspond to proliferating, prehypertrophic, and hypertrophic zones of the growth plate and are magnified in E–J′′. The arrowheads in G′ and H′ indicate perturbed column formation of prehypertrophic chondrocytes in *δ-EF1*–null mice as compared with WT mice. The brackets in G′′ and H′′ indicate columnar stacks. The black and yellow lines in I′–J′′ indicate the size of the hypertrophic zone in WT and *δ-EF1*–null mice, respectively. Note the disturbed columnar organization as well as the reduced size of prehypertrophic and hypertrophic zones in *δ-EF1*–null mice. (K–K′′) Measurements of the different cartilage zones in WT (black) and *δ-EF1*–null mice (gray; *n* = 4 embryos, 5 measurements per embryo in each group; error bars indicate mean ± SD, student's *t* test; *, P < 0.0001). Bars: (A–D′′) 500 µm; (E–J′′) 100 µm.

(markers for nonhypertrophic and hypertrophic chondrocytes, respectively). The *Col2a1* mRNA expression domain was considerably longer in *δ-EF1*–null mice as compared with WT littermates (Fig. 2, A and B, compare red and black lines). Conversely, the *Col10a1* mRNA expression domain was smaller in *δ-EF1*$^{-/-}$ mice (Fig. 2, C and D, compare red and black lines), which suggests a delay in the onset of hypertrophic differentiation in the *δ-EF1*–null embryos. The expression domain of *Col1a1* mRNA (an ossification marker) was reduced (Fig. 2, E and F, compare red and black lines), and mineralization was delayed as visualized by von Kossa staining (Fig. 2, G and H). The osteoblast precursors were, however, present in the perichondrium, as indicated by alkaline phosphatase staining (unpublished data).

The defects in chondrocyte maturation prompted us to examine the expression of genes associated with *Ihh* signal transduction. We analyzed the mRNA's expression of *Ihh* and its receptor and target *Ptc*, as well as *PTHrP* and *PPR*. *Ihh* mRNA expression was maintained in the prehypertrophic and hypertrophic zones but had a broader expression domain as compared with WT littermates (Fig. 2, I and J, compare red and black arrows). *Ptc* mRNA was detected in the perichondrium adjacent to the expression domain of *Ihh* and in the zone of proliferating chondrocytes. Interestingly, in *δ-EF1*$^{-/-}$ mice, the domain of *Ptc* mRNA expression was extended toward the epiphyses (Fig. 2, K and L). The expression of *PPR* was broadened in *δ-EF1*$^{-/-}$ limbs as compared with WTs (Fig. 2, M and N). *PTHrP* expression was detected in round chondrocytes at the ends of long bones of the WT limbs (Hilton et al., 2007), but there was a marked increase in *PTHrP* expression around the epiphyses of the long bones of *δ-EF1*$^{-/-}$ mice (Fig. 2, O and P,

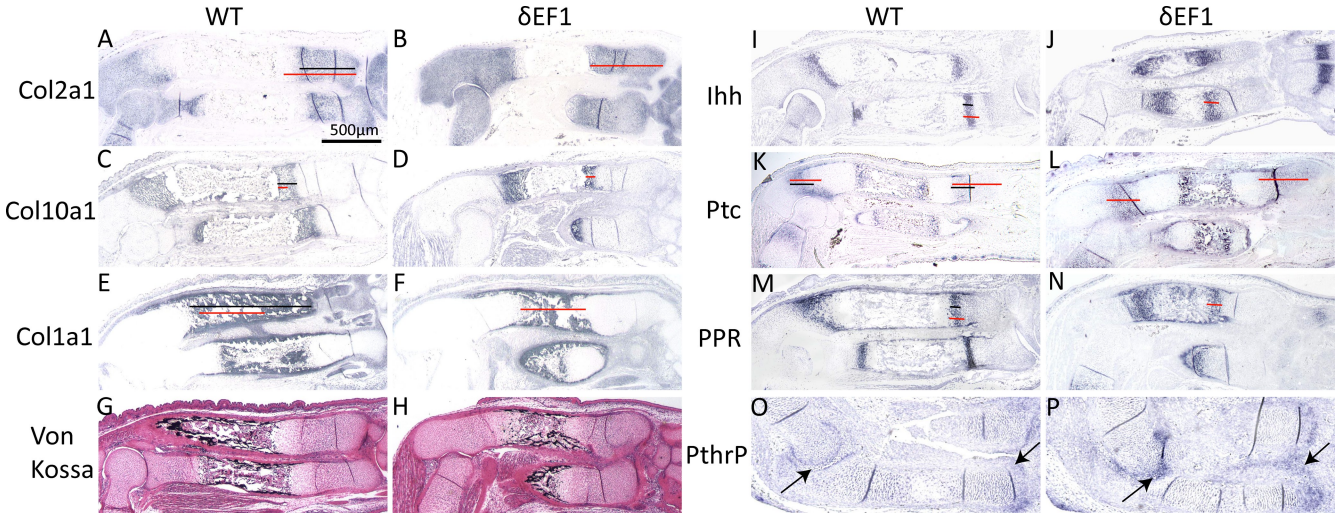

Figure 2. **Hypertrophic differentiation is delayed in *δ-EF1* KO mice.** (A–F and I–P) In situ hybridization for different growth plate markers (named to the left) on the radius and ulna of 14.5-dpc (O and P) and 16.5-dpc (A–N) WT and *δ-EF1* KO limbs. (A and B) The zone of *Col2a1* mRNA expression is expanded in *δ-EF1*$^{-/-}$ mice as compared with WT (black line, WT; red line, *δ-EF1* KO throughout this figure). (C and D) The region of *Col10a1* mRNA–expressing cells is reduced in *δ-EF1*$^{-/-}$ mice. (E and F). *Col1a1* mRNA expression is reduced in *δ-EF1*$^{-/-}$ mice. (G and H) Von Kossa staining of WT (G) and *δ-EF1*$^{-/-}$ limbs (H) showing a delay in bone mineralization in *δ-EF1*$^{-/-}$ mice. (I and J) The domain of *Ihh* mRNA expression is broadened. (K and L) The domain of *Ptc* mRNA expression is expanded in *δ-EF1*$^{-/-}$ limbs as compared with WT limbs. (M and N) *PPR* mRNA expression is broader in *δ-EF1* KO mice as compared with WT mice (O and P). *PTHrP* mRNA expression on 14.5-dpc forelimbs is increased in *δ-EF1*$^{-/-}$ limbs as compared with WT limbs (arrows).

arrows). The changes in the expression pattern of the above-mentioned molecular markers were the same in all long bones examined (unpublished data). In summary, *δ-EF1* deficiency resulted in a delay of chondrocyte hypertrophic differentiation.

δ-EF1 expression in the growth plate

Because *δ-EF1*–null mice have apparent defects in the growth plates of the long bones, we decided to reexamine *δ-EF1* transcripts during bone development. Previous studies showed *δ-EF1* mRNA expressed in the perichondrium of long bones at 14.5 dpc (Takagi et al., 1998; Tylzanowski et al., 2003). Our analysis has revealed additional expression domains of *δ-EF1* mRNA in the growth plate on sections of 14.5 dpc (Fig. 3) and 16.5 dpc (not depicted) mouse embryos using two independent in situ hybridization methods: colorimetric (Fig. 3, A and B) and fluorescent (Fig. 3, C and D). *δ-EF1* transcripts were detected in the entire growth plate (Fig. 3, A and C, red arrows) as well as in some muscles (Fig. 3 A, black arrow; and Fig. 3 C, white arrow; Funahashi et al., 1993). We did not detect expression of *δ-EF1* mRNA in limbs of *δ-EF1*$^{-/-}$ mice (Fig. 3, B and D). The expression of *δ-EF1* mRNA became weaker toward the zone of hypertrophic chondrocytes (Fig. 3 A). These findings indicate that *δ-EF1* mRNA is located at the appropriate place and time during bone development in mice to regulate growth plate differentiation.

Increased chondrocyte proliferation in δ-EF1$^{-/-}$ cartilage

δ-EF1$^{-/-}$ mice display an enlarged zone of resting and proliferating chondrocytes. Because this could have been caused by enhanced proliferation, we analyzed the expression of Ki67, an acknowledged molecular marker of that process. There was a significant increase in the number of cells positive for Ki67 in the proliferative zone (both in noncolumnar and columnar cells) of *δ-EF1*$^{-/-}$ mice as compared with WT littermates (Fig. 4, A–B′) at 16.5 dpc. The number of proliferating cells in the humerus of the mutant was ∼50% higher than in WT mice (Fig. 4 C). Thus, in the absence of *δ-EF1*, the balance between proliferation and differentiation of chondrocytes was changed with a higher rate of chondrocyte proliferation.

Ihh expression is affected in δ-EF1 mutants

Having demonstrated that *δ-EF1*–null mice show an increased cell proliferation in the growth plate, we decided to analyze the expression of *Ihh* during chondrogenesis in detail. In WT mice at 15.5 dpc, IHH protein was detected in prehypertrophic and hypertrophic chondrocytes, and no IHH-positive cells were detected in the domains of resting and proliferating chondrocytes (Fig. 5, A and A′; Koziel et al., 2004). In *δ-EF1*$^{-/-}$ mice, however, a significant amount of IHH-positive cells was detected in the proliferating region of *δ-EF1*$^{-/-}$ mice, and IHH-positive cells were detected in the entire growth plate (Fig. 5, B and B′). Similar results were obtained at 14.5 and 16.5 dpc (unpublished data). To analyze the dynamics of IHH and δ-EF1 protein expression during limb development, we performed Western blot analysis (Fig. 5 C). δ-EF1 was detected from 12.5 dpc, with the expression peak at 14.5 dpc. From 16.5 dpc, δ-EF1 expression could no longer be detected. IHH protein expression was detected from 12.5 dpc onwards, and the expression increased over time. IHH expression in δ-*EF1*$^{-/-}$ limbs was higher as compared with the corresponding stages of WT limbs (Fig. 5 C′, * and ^), confirming the immunohistochemistry data. Quantification of the Western blot bands showed a twofold increase in *Ihh* expression in *δ-EF1*$^{-/-}$ limbs at 13.5 dpc as compared with WT, and a 1.5-fold increase at 18.5 dpc (Fig. 5 C′).

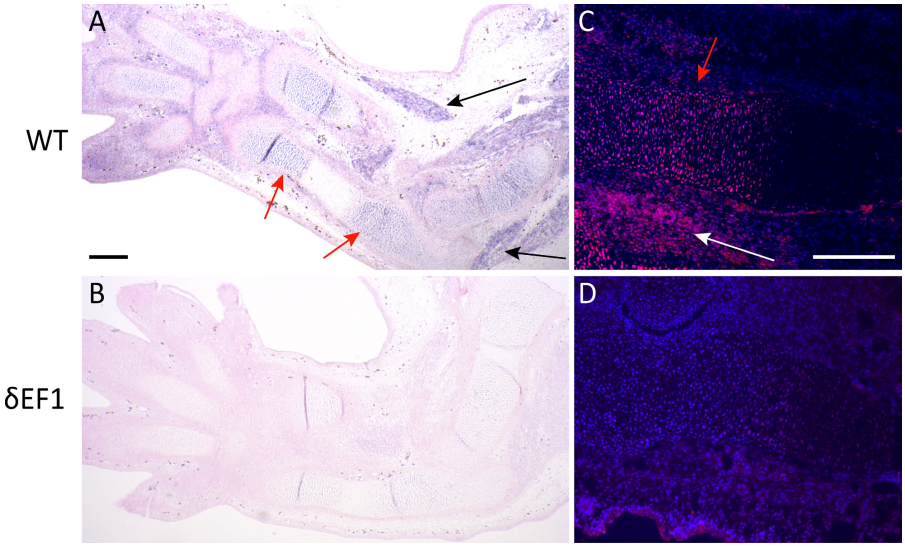

Figure 3. **δ-*EF1* mRNA expression.** In situ hybridization (A and B, colorimetric-positive signal blue; C and D, fluorescent-positive signal red) for δ-*EF1* on longitudinal sections of 14.5-dpc WT (A and C) and δ-*EF1* KO limbs (B and D). δ-*EF1* mRNA is expressed in WT limbs in the growth plate (red arrows in A and C) and certain muscles (black and white arrows in A and C). No δ-*EF1* mRNA expression could be detected in δ-*EF1* KO limbs (B and D). Bars, 100 μm.

Because there was a limited expansion of the *Ihh* mRNA expression domain (as shown in Fig. 2), we measured *Ihh* mRNA expression by quantitative PCR. *Ihh* mRNA expression in the developing limbs was increased in δ-*EF1*$^{-/-}$ mice at all stages from 12.5 dpc onwards, with a peak at 14.5 dpc (Fig. 5 D). These results show that even though the expression domain of *Ihh* mRNA was only slightly expanded, transcription levels of *Ihh* were increased. Importantly, a similar increase in expression of *Ihh* target gene *Ptc* was detected in δ-*EF1*$^{-/-}$ limbs (Fig. 5 E), which supports the notion that the increase in *Ihh* transcription may have biological consequences in vivo.

Ihh has both *PTHrP*-dependent and independent effects on growth plate development. To determine if the defects seen in the growth plates of δ-*EF1*–null mice were *PTHrP* mediated, we analyzed the expression of *PTHrP* mRNA. Similar to *Ihh* and *Ptc*, the mRNA expression of *PTHrP* was increased in δ-*EF1*$^{-/-}$ limbs at all stages (Fig. 5 F) as compared with WT controls.

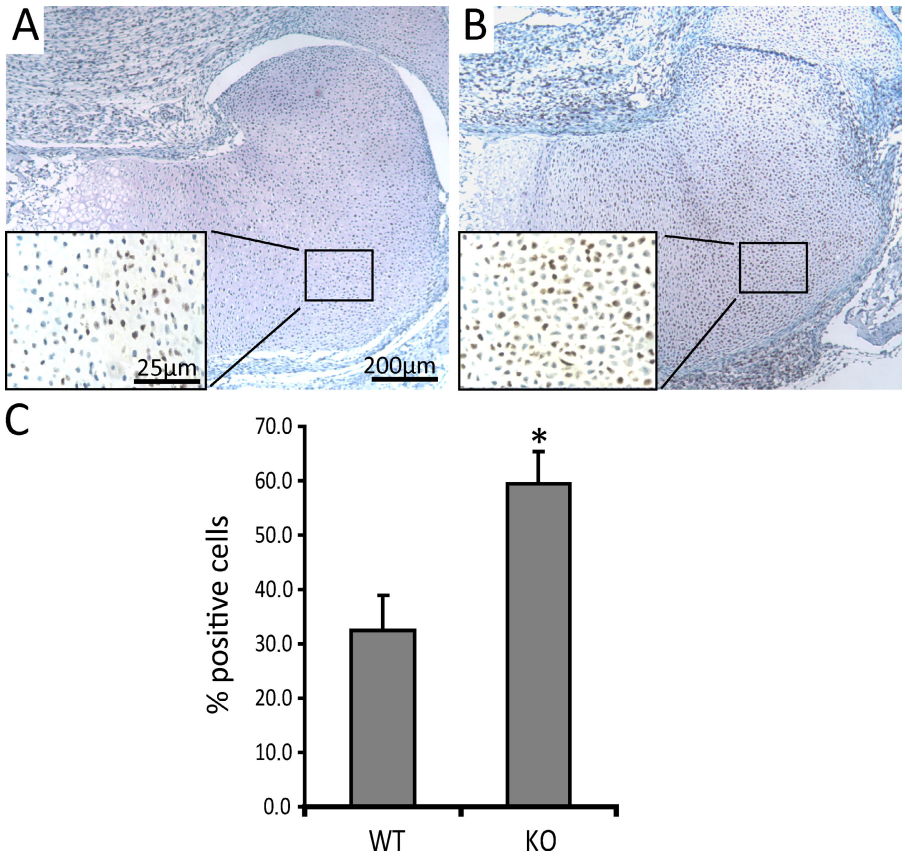

Figure 4. **Increased proliferation in the growth plate of δ-*EF1*–null mice.** Immunohistochemistry for Ki67 in the humerus of WT (A) and δ-*EF1*–null mice (B) at 16.5 dpc. The black rectangle denotes the area magnified in the insets. (C) There are more proliferating cells in δ-*EF1* KO mice as compared with WT (n = 20; the y axis shows the percentage of Ki67-positive cells compared with the total cell number in selected area; bars indicate ±SD, Student's t test; *, $P < 0.00001$).

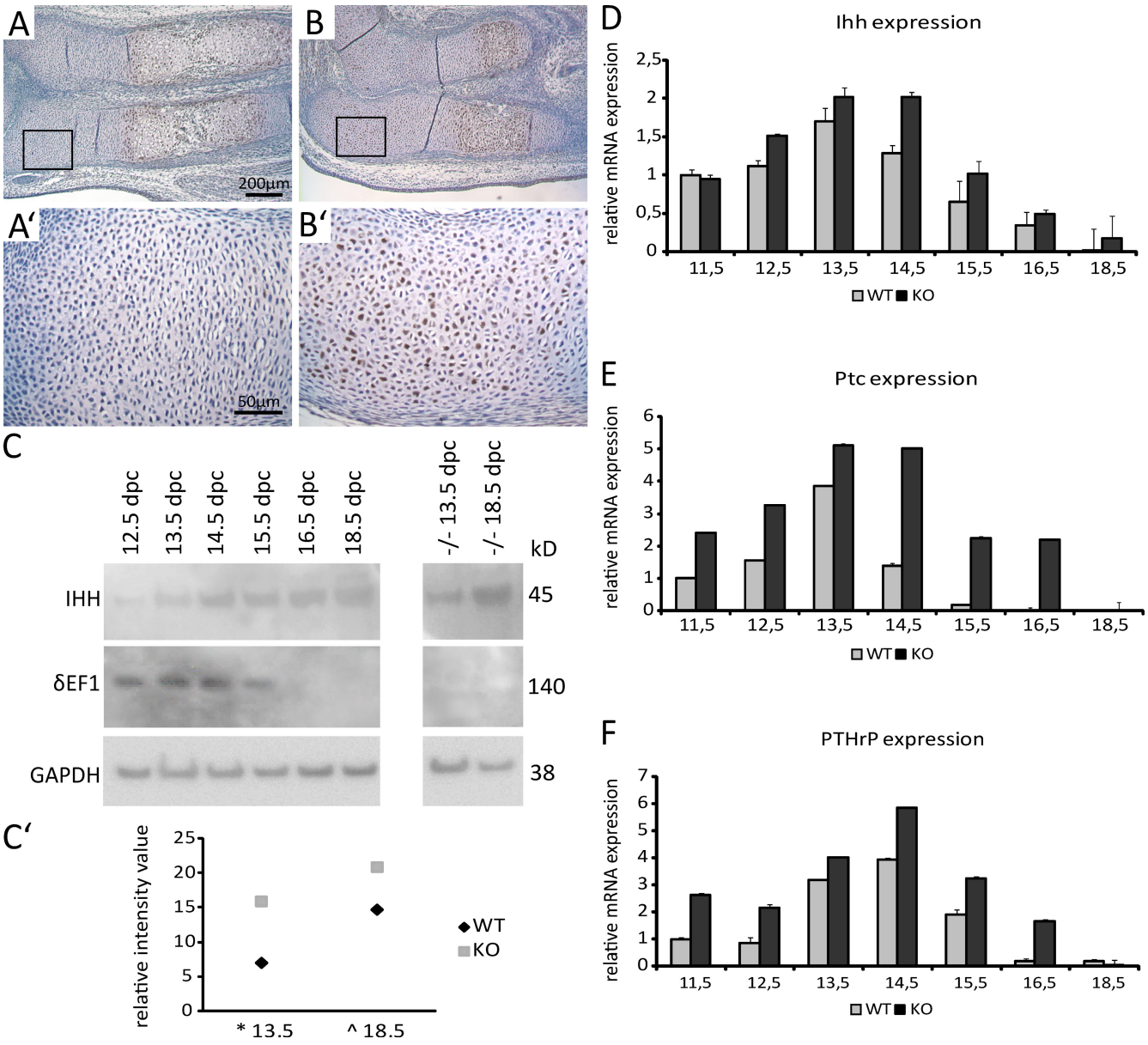

Figure 5. ***Ihh* expression in *δ-EF1*–null mice.** (A–B′′) Immunohistochemistry for *Ihh* shows the presence of IHH in the resting and proliferating regions of *δ-EF1*$^{-/-}$ mice (magnified view in A′ and B′, indicated by black boxes in A and B). (C) Western blot analysis for IHH, δ-EF1, and glyceraldehyde 3-phosphate dehydrogenase (GAPDH) on limb extracts of different stages of WT (left) and δ-EF1$^{-/-}$ (right) mice. * and ^ indicate the IHH expression at 13.5 and 18.5 dpc, respectively; quantification of these Western blot bands by densitometry analysis is shown in C′. (D–F) Quantitative PCR for *Ihh*, *Ptc*, and *PTHrP* on limb lysates of different stages of embryonic development of WT (gray) and *δ-EF1* KO mice (black). Each bar represents a pool of 10 limbs. Samples were normalized to the geometric mean of three housekeeping genes (GAPDH, Hprt1, and β2-microglobulin). Bars represent levels (±SD) of expression relative to WT 11.5 dpc.

In conclusion, deficiency of *δ-EF1* leads to higher levels of *Ihh* mRNA expression and increased IHH protein levels.

δ-EF1 binds in vitro and in vivo to *Ihh*

Because the *δ-EF1*–null phenotype in mice was reminiscent of phenotypes associated with perturbed IHH signaling, we investigated if δ-EF1 could bind directly to regulatory regions of the *Ihh* gene. Indeed, we found four putative δ-EF1 binding sites in a region of 160 bp at the 5′ end of intron 1 of the mouse *Ihh* gene (Fig. 6 A).

One of the indications of a potential functional significance of DNA sequences located in noncoding regions of DNA is their evolutionary conservation across species. Therefore, we aligned the genomic sequence of the mouse *Ihh* to rat, human, dog, cow, chimp, and chicken *Ihh* sequences using VISTA software (Dubchak et al., 2000; Frazer et al., 2004). We found that the 160-bp region in the *Ihh* gene containing putative δ-EF1 binding sites was highly conserved across species (Fig. 6 B, black box).

Next, we investigated if δ-EF1 could bind to these sequences in vitro carrying out electrophoretic mobility shift assay (EMSA) using amino-terminally tagged myc–δ-EF1 and a 65-bp fragment of the mouse *Ihh* intron 1 containing CACCT/CACCTG

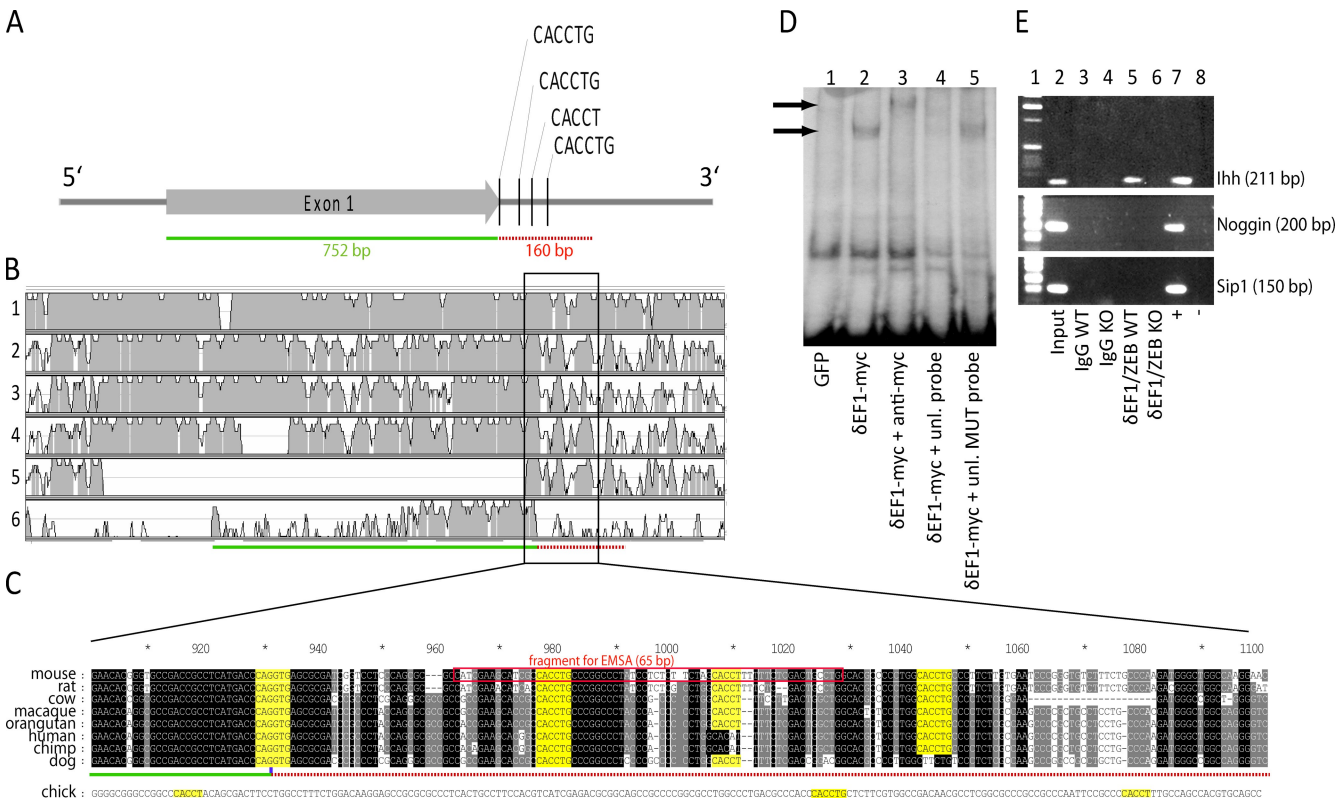

Figure 6. ***δ-EF1* binds to the *Ihh* intron 1 regulatory region in vitro and in vivo.** (A) Schematic representation of the Exon 1/Intron 1 junction of the *Ihh* gene. Exon 1 is indicated by a gray arrow (752 bp). Four CACCT(G) putative binding sites in the 5′ end of intron 1 are indicated. The green line and red dotted line in A, B, and C correspond to exon 1 (green line) and intron 1 (red dotted line). (B) Alignment of the genomic DNA of *Ihh* for different species (mouse compared with 1, rat; 2, human; 3, dog; 4, cow; 5, chimp; and 6, chicken). The region in the black rectangle corresponds to the region with the CACCT(G) binding sites and is strongly conserved across species (gray peaks). (C) A sequence alignment of exon 1/intron 1 junction. CACCT(G) binding sites are indicated in yellow. The chick sequence with binding sites indicated is located below the exon 1/intron 1 schematic drawing. Black background and white letters indicate 100% identity, gray background and white letters indicate >80% identity. The fragment of 65 bp used for EMSA is indicated with a red rectangle. Numbers indicate position on the chromosome. (D) EMSA for binding of δ-EF1 to a selected region of the *Ihh* intron 1 regulatory region of 65 bp (indicated in red in C; the primer sequence to generate the fragment is described in Materials and methods). In each lane, a γ-^{32}P-labeled probe was added to extract of cells transfected with GFP (lane 1) or δ-EF1 (lanes 2, 3, 4, and 5). Lane 3, supershift after adding δ-EF1 monoclonal anti-Myc antibody; lane 4, competition with a 20-fold unlabeled probe; lane 5, no competition with 20-fold unlabeled probe with mutant CACCT(G) binding sites: CATCT(G). Arrows indicate shift (lane 2) and supershift (lane 3). (E) ChIP assay for in vivo binding of δ-EF1 to *Ihh* done on lysates from WT and *δ-EF1* KO limbs. Lane 1, molecular weight marker; lane 2, input DNA; lane 3, IgG negative control on WT cell lysates; lane 4, IgG negative control on *δ-EF1*$^{-/-}$ lysates; lane 5, ChIP assay using δ-EF1–specific antibodies (ZEB) on WT cell lysate; lane 6, ChIP assay using δ-EF1–specific antibodies (ZEB) on *δ-EF1*$^{-/-}$ cell lysate; lane 7 and 8, positive (genomic DNA) and negative (water) PCR control, respectively. (top) Detection of a fragment of the *Ihh* regulatory region of 211 bp containing the selected region by PCR with specific primers (lane 5). (middle and bottom) Control PCRs for unrelated genomic sequences (Noggin and Sip1, respectively) to demonstrate specificity of δ-EF1 binding to the *Ihh* first intron. No *Ihh* fragment was detected after precipitation using δ-EF1–specific antibodies (ZEB; lane 5).

sites as a probe (see Fig. 6 C and Materials and methods). We could demonstrate that myc–δ-EF1 could bind to the intron 1 fragment of *Ihh* (Fig. 6 D). Next, we confirmed the specificity of myc–δ-EF1 binding by carrying out a supershift of the δ-EF1 band with a monoclonal anti-myc antibody (Fig. 6 D, lanes 2 and 3). To verify that the binding was dependent on the presence of the intact bipartite CACCT…CACCTG motif, we performed competition assays. As can be seen on Fig. 6 D (lane 4), the WT *Ihh* fragment competed for δ-EF1 binding with 20-fold the molar excess of the WT, unlabeled, probe. The CA**T**CT…CA**T**CTG mutant (CACCT(G) binding sites are underlined, point mutations in mutated constructs are shown in bold; Fig. 6 D, lane 5) was unable to compete for binding to δ-EF1.

Collectively, the results in Fig. 6 C show that δ-EF1 can bind to the *Ihh* intron 1 fragment in vitro and that this binding is dependent on the presence of an intact bipartite CACCT/CACCTG binding site.

Although EMSA provides the information about the ability of a transcription factor to bind to its target sequence, it does not indicate if such a binding takes place in vivo and is therefore biologically relevant. To address this issue, we have performed chromatin immunoprecipitation (ChIP) experiments. We have designed PCR primers encompassing the 160-bp region containing δ-EF1 putative binding sites in the *Ihh* intron 1 and performed ChIP analysis on 16.5-dpc mouse embryos. After protein cross-linking to DNA, we performed immunoprecipitation using δ-EF1–specific antibodies (ZEB; Eger et al., 2005). As can be seen in Fig. 6 E, we were able to amplify the *Ihh* intron 1 fragment in the DNA templates obtained after immunoprecipitation with anti-δ-EF1 (ZEB) antibodies but not from the IgG controls. Importantly, we did not detect any PCR product in

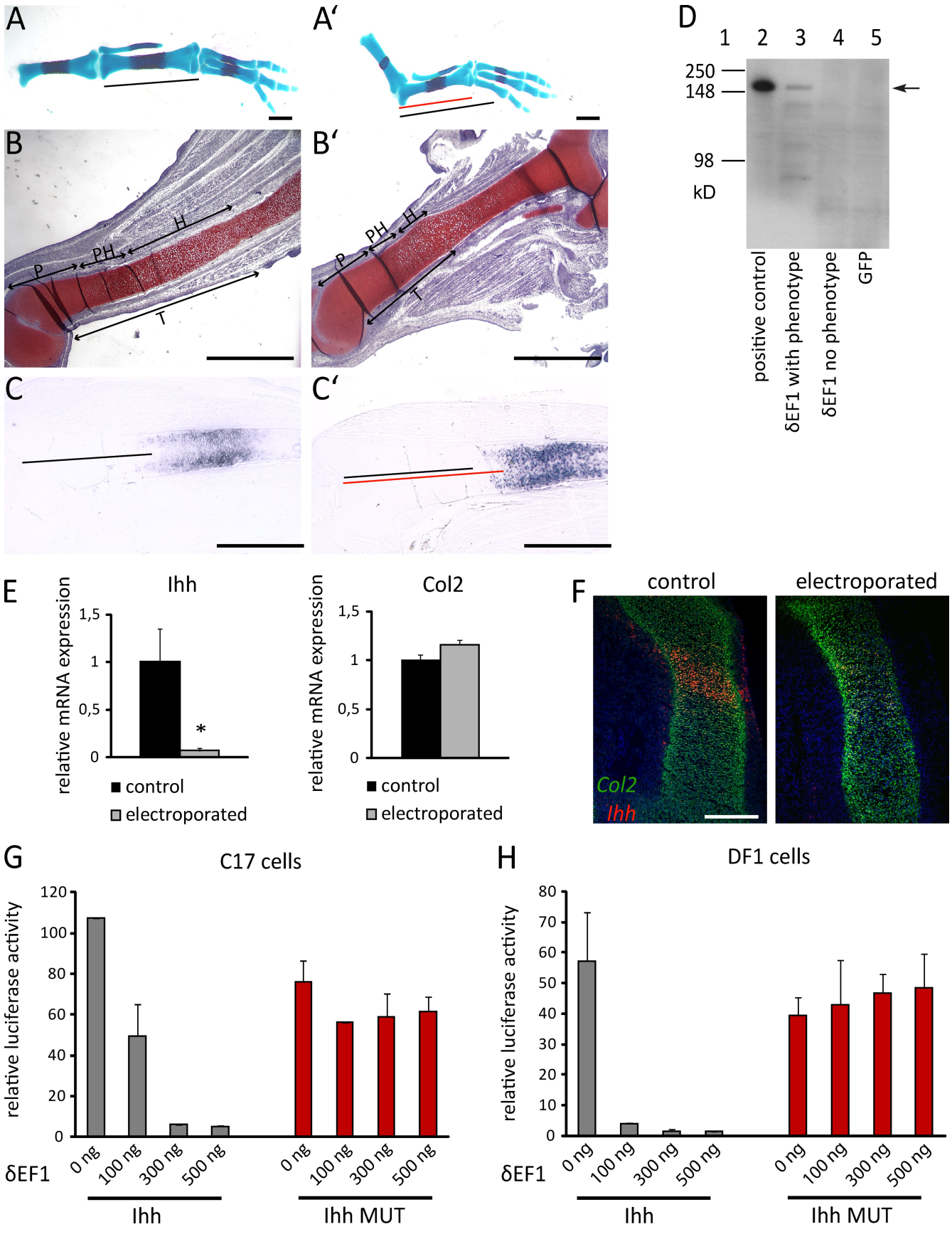

Figure 7. **δ-EF1 negatively regulates *Ihh* expression.** (A–A′) Misexpression of δ-EF1 in developing chick limbs. Skeletal stainings of chick limbs HH stage 37 electroporated with chick *δ-EF1* cDNA (A′) as compared with the contralateral limb (A). The length of the long bones of limbs electroporated with *δ-EF1* cDNA is shorter as the contralateral limbs (compare the red bar in A′ with the black bar in A and A′). (B and B′) Safranin O staining at HH stage 37 of

the lysate obtained from *δ-EF1*–null mice. As seen in the lower panels of Fig. 6 E, we did not detect the presence of unrelated genomic sequences (noggin and Sip1), which ruled out the possibility that the chromatin containing *Ihh* intron 1 was pulled down nonspecifically with δ-EF1 containing chromatin. These results strongly support the notion that intact δ-EF1 binds in vivo to cognate target sequences present in intron 1 of *Ihh*.

Misexpression of δ-EF1 in developing chick limbs results in growth plate defects and decreased IHH signaling

We demonstrated that binding of δ-EF1 to *Ihh* intron 1 takes place both in vitro and in vivo; however, whether this binding would repress or activate gene transcription remained unresolved. Therefore, we performed gain-of-function experiments by misexpressing myc–*δ-EF1* cDNA in developing chick limbs. Chick limbs of Hamburger-Hamilton (HH) stage 18–20 were electroporated with myc–*δ-EF1* in a pCS3 expression construct and incubated until HH stage 36–37, when a skeletal staining was performed. Limbs electroporated with *δ-EF1* construct were reduced in size as compared with the contralateral control limbs or limbs electroporated with empty expression vector (Fig. 7, A and A′; and not depicted). The length of the long bones was reduced by a mean of 25% in the zeugopod and by a mean of 40% in the stylopod, as compared with control limbs electroporated with pCS3 alone at the same developmental stage. Additionally, in some limbs, a small reduction in length of the autopod was detected (unpublished data).

To evaluate if the *δ-EF1* cDNA was successfully expressed in the chick limb, we performed a Western blot analysis on protein samples obtained from electroporated chick limbs using anti-myc primary antibody. Western blot analysis of the cell lysate of transfected limbs, as well as DF1 cells transfected with the same expression construct, revealed a band of 140 kD. Importantly, we could detect δ-EF1 in the cell lysates from limbs that did show the phenotype but could not detect it in the limbs electroporated with *δ-EF1* expression construct but not having the above described phenotype (Fig. 7 D), which supports the notion that the observed phenotype was directly correlated with the successful expression of δ-EF1.

Histologically, the limbs electroporated with *δ-EF1* cDNA showed a significant reduction of the zone of hypertrophic chondrocytes, and bone formation was delayed (Fig. 7, A, A′, B, and B′). Furthermore, the distance between the epiphysis and the zone of hypertrophic chondrocytes, as indicated by *Col10a1* mRNA expression, is enlarged in limbs electroporated with *δ-EF1* cDNA (Fig. 7, C and C′). These observations suggested a delayed onset of hypertrophic and osteogenic differentiation and therefore a possible defect in *Ihh* signaling induced by misexpression of *δ-EF1*. To investigate this hypothesis, we performed quantitative PCR to measure *Ihh* expression levels. Limbs electroporated with *δ-EF1* cDNA showed a significant reduction in *Ihh* expression (Fig. 7 E). To analyze the specificity of this repression, we tested the expression of *Col2a1*, which is negatively regulated by δ-EF1 in vitro (Murray et al., 2000). *Col2a1* mRNA expression was unchanged in *δ-EF1* electroporated limbs as compared with control limbs (Fig. 7 E). Therefore, in spite of *δ-EF1* overexpression in the entire limb bud of developing chicks, the in vivo repressor effect of *δ-EF1* was specific, affecting *Ihh* expression in the growth plate but not another in vitro identified target gene *Col2a1*. These results were confirmed using dual in situ hybridization for *Col2a1* and *Ihh*. Limbs electroporated with *δ-EF1* cDNA showed a significant reduction in *Ihh* mRNA expression (Fig. 7 F, red), whereas expression of *Col2a1* mRNA was unchanged (Fig. 7 F, green). The overexpression of *δ-EF1* cDNA in developing chick limbs provides strong evidence for a role of δ-EF1 as negative regulator of *Ihh* in the growth plate. To further confirm that δ-EF1 negatively regulates expression of the *Ihh* gene, we tested whether δ-EF1 interacts in the transcriptional control of *Ihh* expression. We therefore cotransfected reporter plasmids containing the *Ihh* intron 1 regulatory region with a δ-EF1 expression plasmid. Overexpression of δ-EF1 in both C17 mouse limb bud cells and DF1 chicken fibroblasts consistently inhibited the activity of the *Ihh* intron 1 reporter construct (Fig.7, G and H). δ-EF1 could not, however, inhibit the activity of the construct with mutated CACCT(G) binding sites, which indicates that the intact CACCT(G) δ-EF1 binding sites are required for this activity (Fig. 7, G and H).

δ-EF1 haploinsufficiency causes a postnatal increase in trabecular bone mass

We have demonstrated that the skeletal phenotype of *δ-EF1*$^{-/-}$ embryos was caused by a disturbed *Ihh* signaling. Several studies implicate *Ihh* in postnatal bone homeostasis (Maeda et al., 2007; Mak et al., 2008; Ohba et al., 2008). Therefore, we investigated if deficiency of *δ-EF1* would lead to a postnatal bone phenotype. Because homozygous mutants die at birth, we analyzed 20-wk-old *δ-EF1* heterozygous (HZ) mice. The radiographical analysis revealed normal skeletal patterning in δ-EF1$^{+/-}$ mice

tibia of chicken electroporated with chick *δ-EF1* cDNA. P, proliferating; C, prehypertrophic; H, hypertrophic chondrocytes; T, total length of the growth plate. (C and C′) In situ hybridization for *cCol10a1* at HH39 on tibia of chicks electroporated with chick *δ-EF1* cDNA and control limbs. The black and red lines indicate the distance from the epiphysis to the zone of hypertrophic chondrocytes in the control limbs and limbs electroporated with *δ-EF1* cDNA, respectively. (D) Western blot analysis of the lysate of electroporated limbs with anti-myc antibody. Lane 1, representation of molecular weight marker; lane 2, lysate obtained from DF1 chick cell fibroblasts transfected with chick *δ-EF1* cDNA; lane 3, lysate of limbs electroporated with *δ-EF1* cDNA showing a phenotype; lane 4, lysate of limbs electroporated with *δ-EF1* cDNA not showing a phenotype; lane 5, lysate of limbs electroporated with GFP cDNA. The arrow indicates the position of the positive band on the gel. (E) Quantitative PCR analysis of electroporated limbs shows a down-regulation of *Ihh* mRNA in limbs electroporated with *δ-EF1* cDNA, whereas *Col2a1* mRNA expression was unchanged ($n = 6$, Student's t test; *, $P < 0.00001$; relative expression is normalized to β-actin). (F) Dual in situ hybridization for *Col2a1* (green) and *Ihh* (red). Chick limbs of HH30 electroporated with *δ-EF1* show a decreased *Ihh* expression as compared with contralateral control limbs. (G and H) Effects of *δ-EF1* on the transcriptional activity of *Ihh* intron 1 construct. Luciferase reporter constructs containing WT or mutated *δ-EF1* binding sites from *Ihh* intron 1 were cotransfected into cultured C17 (C) or DF1 (D) cells with either a *δ-EF1* expression vector or empty vector in different concentrations (indicated below the graph). Bars in the graphs indicate relative luciferase activity normalized to β-galactosidase activity, presented as mean ± SD, $n = 3$. Bars: (A–C′) 1 mm; F, 100 µm.

Table I. **DEXA analysis of WT and δ-EF1$^{+/-}$ mice**

Parameter	WT	δ-EF1 HZ
DEXA_total BMD (mg/cm^2)	0.063 ± 0.004	0.068 ± 0.003[a]
DEXA_total BMC (g)	0.674 ± 0.085	0.764 ± 0.039[a]
DEXA_total area (cm^2)	10.554 ± 0.859	11.221 ± 0.505
DEXA_lean (g)	38.758 ± 3.700	40.940 ± 2.978
DEXA_fat (g)	15.531 ± 2.718	15.623 ± 4.414

DEXA of WT and *δ-EF1*$^{+/-}$ (HZ) mice. *n* = 8 animals/group; data presented as mean ± SD; Student's *t* test. BMC, bone mineral content; BMD, bone mineral density.
[a]p < 0.05.

(unpublished data). Next, we performed whole-body dual energy x-ray absorptiometry (DEXA) measurements of muscle, bone, and fat content. This analysis revealed a significant increase in bone mineral density and bone mineral content as compared with WT mice (Table I), and no difference in muscle and fat mass. Peripheral quantitative computed tomography (pQCT) analysis detected a significant increase in the bone trabecular content and trabecular density in *δ-EF1*$^{+/-}$ mice (Table II). To analyze if these observations could be associated with a change in *Ihh* expression, we performed quantitative PCR on dissected growth plates of 8-wk-old WT and *δ-EF1* HZ mice. *Ihh* mRNA expression was significantly up-regulated in growth plates of *δ-EF1* heterozygotes as compared with WTs (Fig. 8). Collectively, haploinsufficiency for *δ-EF1* causes up-regulation of *Ihh* in adult growth plates, a higher bone mineral density, and an increase in trabecular bone content.

Discussion

δ-EF1–null mice have defects in the growth plate of the long bones

δ-EF1–null mice exhibit dwarfism and impaired joint formation (Takagi et al., 1998), but no detailed histological analysis of the developing long bones was available. Therefore, after the breeding of mice into a CD1 background, we have reanalyzed the reported phenotype with specific focus on the histology of the growth plate. Despite the delay in expression of *Col10a1*, a marker gene for hypertrophic differentiation, we still observed hypertrophic chondrocytes in the growth plate of *δ-EF1*$^{-/-}$ mice, which indicates that the hypertrophic differentiation was delayed rather than impaired. Additionally, there was an

Table II. **pQCT analysis of WT and *δ-EF1*$^{+/-}$ mice**

Parameter	WT	δ-EF1 HZ
pQCT_trab content (mg)	0.34 ± 0.08	0.41 ± 0.05[a]
pQCT_trab density (mg/cm^3)	211.21 ± 34.64	243.61 ± 36.28[a]
pQCT_trab area (mm^2)	1.61 ± 0.15	1.68 ± 0.13
pQCT_cort content (mg)	2.11 ± 0.40	2.13 ± 0.27
pQCT_cort density (mg/cm^3)	1,195.90 ± 64.46	1,197.31 ± 62.44
pQCT_cort area (mm^2)	1.77 ± 0.31	1.78 ± 0.21
pQCT_cort thickness (mm)	0.31 ± 0.05	0.31 ± 0.03

pQCT of HZ and WT mice. *n* = 8 animals/group; data presented as mean ± SD; Student's *t* test. cort, cortical; tot, total; Trab, trabecular.
[a]p < 0.05.

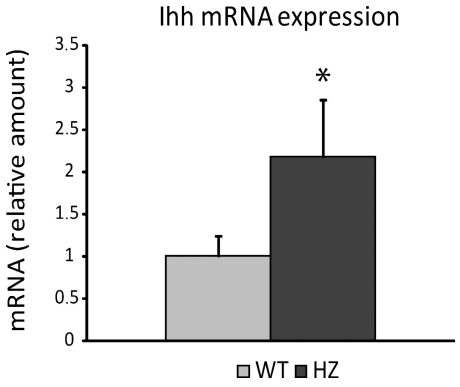

Figure 8. **Haploinsufficiency for *δ-EF1* leads to increased *Ihh* mRNA expression.** Quantitative PCR for *Ihh* on dissected growth plates of 8-wk-old *δ-EF1* HZ mice and WT littermates (*n* = 6 mice per group, Student's *t* test; *, P < 0.01; relative expression normalized to β-actin).

increase in the size of the domain of proliferating chondrocytes and their proliferation rate. Both these defects are consistent with the growth plate phenotypes observed in *Ihh*-null mice (St-Jacques et al., 1999). Conversely, a misexpression of *Ihh* under control of *Collagen type 2* promoter induced *Ptc* mRNA and delayed *Col10a1* mRNA expression (Long et al., 2004). These observations are very similar to our findings in *δ-EF1*–null mice, which suggests a link between δ-EF1 and *Ihh* signaling.

Ihh directly induces proliferation of prehypertrophic chondrocytes (Long et al., 2001). Targeted inactivation of *δ-EF1* leads to significant increase in the proliferation of chondrocytes. Conversely, overexpression of *δ-EF1* in the developing chick limb leads to reduced length of the zone of proliferating chondrocytes. This effect would be expected if the expression levels of *Ihh* would be changed, indicating that the growth plate defects observed in *δ-EF1*$^{-/-}$ mice are consistent with the phenotypes observed after deregulation of *Ihh* expression. Next to the direct effect of *Ihh* on chondrocyte proliferation, *Ihh* also has PTHrP-dependent effects on chondrocyte differentiation. *Ihh* induces the expression of PTHrP in the periarticular perichondrium, which will block hypertrophic differentiation (Vortkamp et al., 1996; Karp et al., 2000). The increase in *Ihh* gene expression in *δ-EF1*–null mice leads to increased PTHrP expression in the periarticular perichondrium. This augmented PTHrP expression is likely to cause the observed delay in hypertrophic differentiation in *δ-EF1*–null mice. In support of our hypothesis, it was recently shown that PTHrP signaling activity is negatively regulated by Wnt/β-catenin signaling to initiate chondrocyte hypertrophy (Guo et al., 2009). In this case, the up-regulation of PTHrP in *δ-EF1*–null mice could be partially counteracted by Wnt/β-catenin signaling, and this could explain a rather mild phenotype of *δ-EF1*–null mice. Furthermore, final maturation of chondrocytes in *δ-EF1*–null mice appears to be less affected, as seen by *Col10a1* mRNA expression. Our data suggest that terminal chondrocyte differentiation is a separate event that is still intact in *δ-EF1*–null mice. This is further supported by the observation that Wnt/β-catenin signaling controls final maturation of chondrocytes independently of PTHrP (Guo et al., 2009).

δ-EF1 negatively regulates *Ihh* expression in the growth plate

Next, we investigated if the observed phenotypes correlated with the changes in *Ihh* gene expression. Both *Ihh* mRNA expression and IHH protein levels were increased in *δ-EF1*$^{-/-}$ mice. These data support our hypothesis that δ-EF1 acts as a negative regulator of *Ihh* transcription in the developing growth plate.

IHH is a long-range signaling molecule and its movement in the growth plate is dependent on heparan sulfate proteoglycans. In mice deficient for glycosyltransferase Ext1, heparan sulfate synthesis is impaired, resulting in an extended range of *Ihh* signaling, as indicated by changes in the expression levels and/or domains of *PTHrP* and *Ptc* mRNAs (Koziel et al., 2004). *Ext1*-null mice have shorter limbs, with joint fusions and defects in hypertrophic differentiation similar to those detected in *δ-EF1*$^{-/-}$ mice. We therefore hypothesize that the excess of IHH protein cannot be sequestered by heparan sulfate, the negative regulator of IHH diffusion. This in turn leads to the extended range of IHH signaling in *δ-EF1*$^{-/-}$ mice and, therefore, phenotypes similar to Ext1 deficiency, including the changes in *PTHrP* and *Ptc* mRNA expression (Koziel et al., 2004).

δ-EF1 binds to the intron 1 regulatory element of *Ihh* in vitro and in vivo

In several genes, intron 1 has been associated with the presence of regulatory elements (Reid et al., 1990; Smith et al., 1996; Antoine and Kiefer, 1998). The *Ihh* gene contains four putative CACCT(G) δ-EF1 binding sites in a very strongly conserved region of intron 1. Our studies demonstrate that δ-EF1 binds to those sequences in vitro and in vivo. The ZFHX1 family of transcription factors is known to be involved in the repression of gene transcription (Funahashi et al., 1993; Kamachi and Kondoh, 1993; Sekido et al., 1994, 1997; Remacle et al., 1999; Comijn et al., 2001; Papin et al., 2002). Binding of δ-EF1 to its target sites in vitro has been demonstrated for several genes (Murray et al., 2000; Terraz et al., 2001; Eger et al., 2005; Jethanandani and Kramer, 2005; Nishimura et al., 2006), and in all these cases, δ-EF1 displayed repressor activity with two exceptions. In one case, δ-EF1 induced ovalbumin expression in estrogen signaling cascades in vitro (Dillner and Sanders, 2004). In the other case, δ-EF1 transactivated promoters of smooth muscle cell differentiation marker genes in vivo (Nishimura et al., 2006).

Here, we demonstrate that δ-EF1 binds to its target sequences in the intron 1 regulatory element of *Ihh* in vivo, implying that it could be involved in transcriptional regulation of *Ihh*. This is a novel and important finding because little is known about the transcriptional regulation of *Ihh* expression. So far, two genes have been reported to directly interact with the *Ihh* promoter in vivo: *Runx2* and *Lef1* (Yoshida et al., 2004; Später et al., 2006). Both of them act as transcriptional activators of *Ihh*, and the identification of a potential in vivo repressor of *Ihh* adds to our understanding of the complex regulatory circuits governing *Ihh* expression.

Misexpression of δ-EF1 in the developing chick limb results in the delay in growth plate maturation

To analyze the effect of δ-EF1 on the transcription of *Ihh*, we have performed luciferase reporter analyses with the *Ihh* regulatory element constructs and a δ-EF1 expression plasmid. We have shown in two different cell lines that δ-EF1 has a negative regulatory effect on *Ihh* transcription. The binding sites for δ-EF1 in the first intron are required for this regulation because a point mutation in the CACCT(G) binding sites prevents this inhibitory effect of δ-EF1 on the *Ihh* transcription. These in vitro experiments clearly indicate that δ-EF1 is a negative regulator of *Ihh* in the growth plate; however, this does not necessarily reflect the in vivo situation. Therefore, in addition to these in vitro experiments, we performed in vivo overexpression of δ-EF1 to analyze the regulatory function of δ-EF1 specifically in the growth plate. The developing chick embryo is a versatile and robust model system to study, among other things, limb development and osteochondrogenic differentiation (Tickle, 2004). Therefore, we have misexpressed *δ-EF1* cDNA in developing chick limbs to investigate the effect on *Ihh* mRNA expression. Indeed, we achieved a reduction in *Ihh* expression in developing chick limbs, which supports the notion that δ-EF1 can repress the expression of *Ihh* in vivo. Moreover, we did not detect changes in expression of *Col2a1*, whereas δ-EF1 has been shown to repress *Col2a1* transcription in vitro (Murray et al., 2000). Although overexpression experiments have their limitations, the target gene–specific response in this case is supportive of our hypothesis that δ-EF1 is repressing *Ihh* transcription in vivo. In chick limbs electroporated with *δ-EF1* cDNA, we observed a reduction in length of the long bones consistent with the *Ihh* knockout (KO) phenotype (St Jacques et al., 1999). *Ihh* KO mice display a dynamic bone phenotype. At 16.5 dpc, they have a delay in calcification, but at 18.5 dpc, this process is enhanced as compared with the WT littermates. The stage at which we analyzed the chick embryos corresponds to the 16.5-dpc stage in the *Ihh* mouse mutants, and the observed delay in calcification is consistent with the mouse phenotype. Additionally, it was demonstrated that infection of developing chick limb bud with Nkx3.2 results in down-regulation of *Ihh* expression, and the bone phenotype is very similar to the one induced by *δ-EF1* cDNA (Provot et al., 2006). Namely, there is restriction of the *Col10a1* expression domain and a delay in hypertrophy. Therefore it is likely that there are aspects of growth plate biology in the chick that are somewhat different than in the mouse. The reason why the induced phenotype is not as pronounced as in the *Ihh*-null mice is most likely caused by the delivery method of *δ-EF1* cDNA. Chick limb electroporation delivers DNA to target tissues with variable efficiency, and although our system has been optimized for high efficiency using GFP expressing vectors, it is unlikely that we are able to target all the cells in the developing limb. Consequently, some cells will escape δ-EF1 repression, causing a milder limb phenotype. Another way of misexpressing genes in developing chick is by using RCAS virus-based system. Although the system is very efficient and effective, it has a major limitation

in the size of the open reading frame that can be misexpressed, namely ~2.3 kb. Because the *δ-EF1* open reading frame is larger than 3 kb, this system cannot be used in our work. Currently, there are no alternative expression systems that could be used in the chick.

δ-EF1 haploinsufficiency leads to increased trabecular bone mass in adult mice

In this paper, we show that haploinsufficiency of *δ-EF1* in mice leads to an increase in the adult bone mass and trabecular bone in a gender-independent fashion. Moreover, we detected up-regulation of *Ihh* expression in the growth plates of 8-wk-old *δ-EF1* HZ mice, which indicates that the increase in trabecular bone could be the result of *Ihh* derepression. Our hypothesis that *δ-EF1* is a repressor of *Ihh* during postnatal bone growth is supported by several findings. It has been shown that defects in Hh signaling cause a range of postnatal mouse phenotypes as well as human disorders affecting skeletogenesis (Maeda et al., 2007; Chen et al., 2008; Lodder et al., 2008). Moreover, it has been recently reported that *Ptc* haploinsufficiency increased adult bone mass in mice (Ohba et al., 2008). Here, the authors have correlated the decrease in *Ptc* expression to ectopic activation of *Smo* and, therefore, activation of *Ihh* signaling. Additionally, it has also been shown that *Ihh* produced in postnatal chondrocytes is essential to maintain the growth plate and specifically the trabecular bone (Maeda et al., 2007). Our observation that a depletion of *δ-EF1* increases trabecular bone is also in line with the studies that both δ-EF1 and *Ihh* are expressed in the growth plate of the late hypertrophic zone and osteoblasts of 8-wk-old mice (Davies et al., 2002), and in early hypertrophic chondrocytes and osteoblasts in mouse, rat, and human growth plates (Iwasaki et al., 1997; Murakami and Noda, 2000; Kindblom et al., 2002; Maeda et al., 2007).

These results suggest that δ-EF1 is involved in the regulation of multiple steps of skeletal development and postnatal homeostasis. We therefore propose that *δ-EF1* acts as a repressor of *Ihh* transcription involved in the determination of the boundaries of *Ihh* expression and expression levels.

In summary, we demonstrate that *δ-EF1* is a novel in vivo regulator of *Ihh* expression in the growth plate. This finding adds to our understanding of growth plate biology and provides new insights into bone development and postnatal bone homeostasis.

Materials and methods

Analysis of mouse embryos

δ-EF1 HZ mice were kindly provided by Y. Higashi (Institute for Developmental Research, Aichi Human Services Center, Osaka, Japan) and moved into a CD1 background. Mouse colonies were maintained according to the National Animal Welfare Guidelines. *δ-EF1*$^{+/-}$ mice in CD1 background (backcrossed >10 times) were mated to generate homozygous *δ-EF1*$^{-/-}$ embryos. The pregnant mice were sacrificed by cervical dislocation. All subsequent mouse work, including skeletal stainings, was performed as described previously (Hogan et al., 2004). For analyses on sections, embryonic tissues were fixed in 4% paraformaldehyde overnight at room temperature and embedded in paraffin before sectioning at 5 µm. Safranin O and von Kossa stainings were performed according to standard protocols. Mouse genotyping was performed by PCR on DNA isolated from yolk sacs (Hogan et al., 2004). The PCR primers used to identify *δ-EF1* WT allele were δ-EF1 S (5′-AGCACTATTCTCCGCTACTCCAC-3′) and δ-EF1 AS (5′-ACCGCACCTGGTTTACGACACTC-3′), generating a fragment of 193 bp. Primers to identify *δ-EF1* null allele were δ-EF1 S as described before and δ-EF1 AS (5′-AACCGTGCATCTGCCAGTTTGAG-3′), generating a fragment of 537 bp.

Immunofluorescence and in situ hybridization

Immunofluorescence was performed using standard protocols using the following primary antibodies: mouse IgG (Biognost), ZEB for detection of δ-EF1 (E-20), IHH (C-15; both from Santa Cruz Biotechnology, Inc.), and TEC-3 for detection of Ki67 (Dako). For analysis of cell proliferation, the ratio of positive cells to the total cell number in a microscopic field was counted (n = 20, with n equal to number of sections; five different embryos). The microscopic field was determined using histological landmarks on a photograph. Subsequent analysis was performed on the photographs. Statistical analysis was performed using an unpaired student's t test.

In situ hybridization was performed on paraffin sections using standard procedures. The mRNA probes (see the Results section) were used as described previously (Koziel et al., 2004; Smits et al., 2004; Später et al., 2006). The δ-EF1 probe was designed using primers CD183-AS (5′-CATATGCTAAATCCGCTTCAG-3′) and CD184-S (5′-GGTCTTGCTTAAGGCCAAAGG-3′; sequence from nucleotide position 3,751–4,160 from GenBank/EMBL/DDBJ under accession no. D76432).

Probes were provided by Christine Hartmann (The Research Institute of Molecular Pathology, Vienna, Austria), Patrick Smits (Harvard University, Boston, MA), Christa Maas (University of Leuven, Leuven, Belgium), and Laetitia Buelens (University of Essen, Essen, Germany).

In ovo electroporation

Fertilized eggs (Poel-Houben) were incubated at 38.5°C in a humidified atmosphere until they reached the desired developmental stage. Chicks were staged using HH staging criteria (Hamburger and Hamilton, 1992). 1 µg/µl DNA + 0.1% fast green was injected multiple times into the hind limb buds of HH stage 18–20 chick embryos. For the expression studies, δ-EF1 cDNA was cloned into a pCS3 vector (Rupp et al., 1994). The ECM 830 ElectroSquarePorator (BTX) was used to generate electric pulses. Two gold-plated electrodes (ϕ = 5 mm) were placed dorsally and ventrally of the limb bud. Electroporation was performed at the following conditions: voltage, 12 V; length of pulse, 50 ms; and frequency, four times.

Quantitative RT-PCR and Western analysis

Limb buds of 12.5–18.5 dpc WT and δ-EF1$^{-/-}$ embryos were removed and homogenized for RNA extraction. 1 µg of each RNA sample was transcribed to cDNA. PCR was performed on a Rotor-gene 6000 detection system (Westburg), and analysis was performed using the accompanied software. For Western blot analysis, samples were homogenized in 60 µl of NuPage sample buffer (Invitrogen). Protein concentration was measured using a BCA Protein Assay Reagent kit (Thermo Fisher Scientific), and 20 µg of protein was loaded per lane. Each sample was mixed with 5 µl 0.5M DTT and denatured for 5 min at 95°C. For detection of injected δ-EF1 in chick limbs, the samples were loaded on a 8% Tris-glycine (Invitrogen) gel, and SDS-PAGE was performed in a Tris-glycine running buffer for 1 h and 30 min at 125 V. 200 µg/ml of anti-myc mouse monoclonal antibody (Sanvertech) diluted 1:500 in TBS with Tween 20 was used to detect injected δ-EF1 in pCS3. For detection of *Ihh* and δ-EF1 in mouse limbs: samples were loaded on a 4–12% Bis-Tris gel (Invitrogen), and electrophoresis was performed in MES running buffer for 1 h and 30 min at 120 V. Primary anti-IHH and anti-ZEB antibodies were diluted 1:200. Densitometry analysis of the Western blot in Fig. 5 was performed using ImageJ software.

EMSA

DNA fragments of 65 bp containing the putative intron 1 regulatory elements of *Ihh* were obtained using the following DNA oligonucleotides in a PCR reaction using mouse genomic DNA as a template (CACCT/CACCTG sites underlined): oligo *Ihh* EMSA: mIhh EMSA S, 5′-CATCGAAGCATCGCCACCTGC-3′; mIhh EMSA AS, 5′-CAGGCAGTCGAGAAAAAAGGTGC-3′. To generate mutated sites, the following primers were used in PCR reactions as described before (mutated base in bold): oligo *Ihh* EMSA mutant: mIhh EMSA S mutant, 5′-CATCGAAGCATCGCCA**T**CTGC-3′; mIhh EMSA AS mutant, 5′-CAGGCAGTCGAGAAAAAAG**A**TGC-3′. Nuclear extracts were prepared from confluent monolayers of DF1 cells transfected with GFP or δ-EF1 in pCS3 using a standard published method (Tylzanowski et al., 2001). 1 µl of nuclear extract was incubated for 40 min at room temperature with γ[^{32}P]ATP end-labeled DNA *Ihh* oligo. Competition analysis was performed with 4- or 20-fold molar excess of unlabeled *Ihh* or *Ihh* mutant DNA fragment. For supershift assays, 1 µl of anti-myc mouse monoclonal antibody (200 µg/ml) was added to the nuclear extract. DNA–protein complexes were separated on a 6% nondenaturing

polyacrylamide gel in 1× Tris-acetate-EDTA, pH 8.5, at 18 mA. The gel was dried and exposed to film (MS; Kodak) for autoradiography.

Reporter assay

WT and mutated 65-bp PCR fragments, as described in the EMSA paragraph, were cloned into the SmaI site of pGL3tk vector (Promega) immediately upstream of a thymidine kinase minimal promoter (modified as described in Verschueren et al., 1999). The cell lines used were C17 cells, an immortalized cell line from a 13.5-dpc limb bud (provided by Vicky Rosen, Harvard University School of Medicine, Boston, MA; Rosen et al., 1993), and DF1 cells, a chicken fibroblast cell line (Cheryl Tickle, University of Bath, Bath, England, UK; Himly et al., 1998). Cells were cotransfected with δ-EF1 expression constructs in pCDNA3 (Remacle et al., 1999) using Fugene HD (Roche) method according to manufacturer's instructions. The amount of transfected DNA was adjusted to a total amount of 600 ng of DNA with the empty expression vector pCDNA3. Luciferase assay was performed 24 h after transfection as described previously (Tylzanowski et al., 2001). As an internal control for transfection efficiency, cells were cotransfected with RSV-LacZ constructs, and β-galactosidase values were determined using a luminescent β-galactosidase assay (Gal-screen; Tropix).

ChIP

Mouse 16.5-dpc limbs were dissected and frozen at −80°C. Between 40 and 60 mg of tissue was ground in a mortar with the base submerged in liquid nitrogen. Cell lysate was fixed for 10 min in 1% formaldehyde in PBS. Chromatin shearing and ChIP assays were performed using the ChIP-IT enzymatic kit according to manufacturer's instructions (Active Motif). Primary antibodies were mouse IgG (Biognost) for negative control and anti-ZEB, as described in the Immunofluorescence and in situ hybridization section. PCR was performed using primers recognizing a 211-bp fragment of the *Ihh* regulatory region: mIhh ChIP S, 5′-ATCCCGACATCATCTTCAAGGACG-3′; mIhh ChIP AS, 5′-CCATCTTGGGCAGAAAGACACCC-3′.

The primers used to identify the Noggin WT allele were Noggin-S (5′-GCATGGAGCGCTGCCCCAGC-3′) and Noggin-AS (5′-GAGCAGCGAGCGCAGCAGCG-3′), generating a fragment of 200 bp. Primers to identify WT allele were SIP1WT-S (5′-ATCAGCAGCCTCCTATTTAAACAGAGTGTC-3′) and SIP1KO-S (5′-GAACTAGTTGAATTGGTAGAATCAATGGGG-3′), generating a fragment of 150 bp. The PCR conditions were annealing at 60°C for 10 s, an extension at 72°C for 20 s, and denaturation at 98°C for 3 s.

DEXA and pQCT

Total body (excluding the head) and lumbar spine bone density and lean and fat body mass were determined by dual x-ray absorptiometry using a Piximus densitometer (Lunar). Trabecular and cortical bone mineral content were assessed by pQCT using an XCT Research M system (Norland Medical Systems). Slices of 0.2 mm in thickness were scanned using a voxel size of 0.07 mm. Three scans were taken 2.4–2.6 mm from the distal end of the femur or 1.4–1.6 mm from the proximal end of the tibia to determine trabecular bone parameters. An additional scan was taken 4 mm from the distal end of the femur or 7 mm from the proximal end of the tibia to determine cortical bone parameters. Statistical analysis was done using a Student's two-sided *t* test.

Digital image acquisition and analysis

Photography of sections was performed using a SPOT2 digital camera (Diagnostic Instruments, Inc.) placed on microscope (DMR; Leica) with the following objectives: a 2.5× (0.07 NA) N-Plan objective and 5× (0.15 NA), 10× (0.30), and 20× (0.50) HC PL Fluotar objectives (all from Leica). Skeletal stainings were photographed using a SPOT Insight camera (Diagnostic Instruments, Inc.) on a stereo microscope (Discovery V8; Carl Zeiss, Inc.) with a 1.0× free working distance 81-mm Plan-S objective or a 0.63× FWD 115-mm Achromat-S objective. Images were taken in TIFF format with SPOT 4.0.8 software (Diagnostic Instruments, Inc.). Small image modifications (brightness, contrast, and color balance) were performed using Photoshop Elements 2.0 (Adobe) on the entire image.

We thank the group of LSD & Joints, Jenny Peeters, and Roel Vandepoel for help with the mouse work; and Scott Roberts, Jeroen Eyckmans, and Rik Lories for helpful suggestions. Thanks to Laetitia Buelens and Eve Seuntjens for help with in situ experiments. We thank all those who kindly provided probes: Christine Hartmann (The Research Institute of Molecular Pathology, Vienna, Austria), Patrick Smits (Harvard University, Boston, MA), Christa Maas (University of Leuven, Leuven, Belgium), and Laetitia Buelens (University of Essen, Essen, Germany). C17 cells were a kind gift from Vicky Rosen (Harvard University School of Medicine, Boston, MA) and DF1 cells were a generous gift from Cheryl Tickle (University of Bath, Bath, England, UK).

This work was funded by FWO G.214.07 and a PhD grant from the Institute for the Promotion of Innovation Through Science and Technology in Flanders (Instituut voor de Aanmoediging van Innovatie door Wetenschap en Technologie in Vlaanderen) to Ellen Bellon.

Submitted: 7 April 2009
Accepted: 23 October 2009

References

Antoine, M., and P. Kiefer. 1998. Functional characterization of transcriptional regulatory elements in the upstream region and intron 1 of the human S6 ribosomal protein gene. *Biochem. J.* 336:327–335.

Bi, W., J.M. Deng, Z. Zhang, R.R. Behringer, and B. de Crombrugghe. 1999. Sox9 is required for cartilage formation. *Nat. Genet.* 22:85–89. doi:10.1038/8792

Bitgood, M.J., and A.P. McMahon. 1995. Hedgehog and Bmp genes are coexpressed at many diverse sites of cell-cell interaction in the mouse embryo. *Dev. Biol.* 172:126–138. doi:10.1006/dbio.1995.0010

Cabanillas, A.M., and D.S. Darling. 1996. Alternative splicing gives rise to two isoforms of Zfhep, a zinc finger/homeodomain protein that binds T3-response elements. *DNA Cell Biol.* 15:643–651. doi:10.1089/dna.1996.15.643

Chen, Y., and G. Struhl. 1996. Dual roles for patched in sequestering and transducing Hedgehog. *Cell.* 87:553–563. doi:10.1016/S0092-8674(00)81374-4

Chen, X., C.M. Macica, A. Nasiri, and A.E. Broadus. 2008. Regulation of articular chondrocyte proliferation and differentiation by indian hedgehog and parathyroid hormone-related protein in mice. *Arthritis Rheum.* 58:3788–3797. doi:10.1002/art.23985

Cohen, M.M. Jr. 2003. The hedgehog signaling network. *Am. J. Med. Genet. A.* 123A:5–28. doi:10.1002/ajmg.a.20495

Colnot, C., L. de la Fuente, S. Huang, D. Hu, C. Lu, B. St-Jacques, and J.A. Helms. 2005. Indian hedgehog synchronizes skeletal angiogenesis and perichondrial maturation with cartilage development. *Development.* 132:1057–1067. doi:10.1242/dev.01649

Comijn, J., G. Berx, P. Vermassen, K. Verschueren, L. van Grunsven, E. Bruyneel, M. Mareel, D. Huylebroeck, and F. van Roy. 2001. The two-handed E box binding zinc finger protein SIP1 downregulates E-cadherin and induces invasion. *Mol. Cell.* 7:1267–1278. doi:10.1016/S1097-2765(01)00260-X

Davies, S.R., S. Sakano, Y. Zhu, and L.J. Sandell. 2002. Distribution of the transcription factors Sox9, AP-2, and [delta]EF1 in adult murine articular and meniscal cartilage and growth plate. *J. Histochem. Cytochem.* 50:1059–1065.

Dillner, N.B., and M.M. Sanders. 2004. Transcriptional activation by the zinc-finger homeodomain protein delta EF1 in estrogen signaling cascades. *DNA Cell Biol.* 23:25–34. doi:10.1089/104454904322745907

Dubchak, I., M. Brudno, G.G. Loots, L. Pachter, C. Mayor, E.M. Rubin, and K.A. Frazer. 2000. Active conservation of noncoding sequences revealed by three-way species comparisons. *Genome Res.* 10:1304–1306. doi:10.1101/gr.142200

Eger, A., K. Aigner, S. Sonderegger, B. Dampier, S. Oehler, M. Schreiber, G. Berx, A. Cano, H. Beug, and R. Foisner. 2005. DeltaEF1 is a transcriptional repressor of E-cadherin and regulates epithelial plasticity in breast cancer cells. *Oncogene.* 24:2375–2385. doi:10.1038/sj.onc.1208429

Franklin, A.J., T.L. Jetton, K.D. Shelton, and M.A. Magnuson. 1994. BZP, a novel serum-responsive zinc finger protein that inhibits gene transcription. *Mol. Cell. Biol.* 14:6773–6788.

Frazer, K.A., L. Pachter, A. Poliakov, E.M. Rubin, and I. Dubchak. 2004. VISTA: computational tools for comparative genomics. *Nucleic Acids Res.* 32:W273–W279. doi:10.1093/nar/gkh458

Funahashi, J., R. Sekido, K. Murai, Y. Kamachi, and H. Kondoh. 1993. Delta-crystallin enhancer binding protein delta EF1 is a zinc finger-homeodomain protein implicated in postgastrulation embryogenesis. *Development.* 119:433–446.

Genetta, T., D. Ruezinsky, and T. Kadesch. 1994. Displacement of an E-box-binding repressor by basic helix-loop-helix proteins: implications for B-cell specificity of the immunoglobulin heavy-chain enhancer. *Mol. Cell. Biol.* 14:6153–6163.

Guo, X., K.K. Mak, M.M. Taketo, and Y. Yang. 2009. The Wnt/beta-catenin pathway interacts differentially with PTHrP signaling to control chondrocyte hypertrophy and final maturation. *PLoS One.* 4:e6067. doi:10.1371/journal.pone.0006067

Hamburger, V., and H.L. Hamilton. 1992. A series of normal stages in the development of the chick embryo. 1951. *Dev. Dyn.* 195:231–272.

Hammerschmidt, M., A. Brook, and A.P. McMahon. 1997. The world according to hedgehog. *Trends Genet.* 13:14–21. doi:10.1016/S0168-9525(96)10051-2

Hilton, M.J., X. Tu, and F. Long. 2007. Tamoxifen-inducible gene deletion reveals a distinct cell type associated with trabecular bone, and direct regulation of PTHrP expression and chondrocyte morphology by Ihh in growth region cartilage. *Dev. Biol.* 308:93–105. doi:10.1016/j.ydbio.2007.05.011

Himly, M., D.N. Foster, I. Bottoli, J.S. Iacovoni, and P.K. Vogt. 1998. The DF-1 chicken fibroblast cell line: transformation induced by diverse oncogenes and cell death resulting from infection by avian leukosis viruses. *Virology.* 248:295–304. doi:10.1006/viro.1998.9290

Hogan, B., R. Beddington, and F.L.E. Constantini. 2004. Manipulating the mouse embryo. Cold Spring Laboratory Press. 487 pp.

Iwasaki, M., A.X. Le, and J.A. Helms. 1997. Expression of indian hedgehog, bone morphogenetic protein 6 and gli during skeletal morphogenesis. *Mech. Dev.* 69:197–202. doi:10.1016/S0925-4773(97)00145-7

Jethanandani, P., and R.H. Kramer. 2005. Alpha7 integrin expression is negatively regulated by deltaEF1 during skeletal myogenesis. *J. Biol. Chem.* 280:36037–36046. doi:10.1074/jbc.M508698200

Kamachi, Y., and H. Kondoh. 1993. Overlapping positive and negative regulatory elements determine lens-specific activity of the delta 1-crystallin enhancer. *Mol. Cell. Biol.* 13:5206–5215.

Karp, S.J., E. Schipani, B. St-Jacques, J. Hunzelman, H. Kronenberg, and A.P. McMahon. 2000. Indian hedgehog coordinates endochondral bone growth and morphogenesis via parathyroid hormone related-protein-dependent and -independent pathways. *Development.* 127:543–548.

Kindblom, J.M., O. Nilsson, T. Hurme, C. Ohlsson, and L. Sävendahl. 2002. Expression and localization of Indian hedgehog (Ihh) and parathyroid hormone related protein (PTHrP) in the human growth plate during pubertal development. *J. Endocrinol.* 174:R1–R6. doi:10.1677/joe.0.174R001

Kobayashi, T., D.W. Soegiarto, Y. Yang, B. Lanske, E. Schipani, A.P. McMahon, and H.M. Kronenberg. 2005. Indian hedgehog stimulates periarticular chondrocyte differentiation to regulate growth plate length independently of PTHrP. *J. Clin. Invest.* 115:1734–1742. doi:10.1172/JCI24397

Koziel, L., M. Kunath, O.G. Kelly, and A. Vortkamp. 2004. Ext1-dependent heparan sulfate regulates the range of Ihh signaling during endochondral ossification. *Dev. Cell.* 6:801–813. doi:10.1016/j.devcel.2004.05.009

Kronenberg, H.M. 2003. Developmental regulation of the growth plate. *Nature.* 423:332–336. doi:10.1038/nature01657

Lanske, B., M. Amling, L. Neff, J. Guiducci, R. Baron, and H.M. Kronenberg. 1999. Ablation of the PTHrP gene or the PTH/PTHrP receptor gene leads to distinct abnormalities in bone development. *J. Clin. Invest.* 104:399–407. doi:10.1172/JCI6629

Lodder, E.M., A.J. Hoogeboom, J.H. Coert, and E. de Graaff. 2008. Deletion of 1 amino acid in Indian hedgehog leads to brachydactylyA1. *Am. J. Med. Genet. A.* 146A:2152–2154. doi:10.1002/ajmg.a.32441

Long, F., X.M. Zhang, S. Karp, Y. Yang, and A.P. McMahon. 2001. Genetic manipulation of hedgehog signaling in the endochondral skeleton reveals a direct role in the regulation of chondrocyte proliferation. *Development.* 128:5099–5108.

Long, F., U.I. Chung, S. Ohba, J. McMahon, H.M. Kronenberg, and A.P. McMahon. 2004. Ihh signaling is directly required for the osteoblast lineage in the endochondral skeleton. *Development.* 131:1309–1318. doi:10.1242/dev.01006

Maeda, Y., E. Nakamura, M.T. Nguyen, L.J. Suva, F.L. Swain, M.S. Razzaque, S. Mackem, and B. Lanske. 2007. Indian Hedgehog produced by postnatal chondrocytes is essential for maintaining a growth plate and trabecular bone. *Proc. Natl. Acad. Sci. USA.* 104:6382–6387. doi:10.1073/pnas.0608449104

Mak, K.K., Y. Bi, C. Wan, P.T. Chuang, T. Clemens, M. Young, and Y. Yang. 2008. Hedgehog signaling in mature osteoblasts regulates bone formation and resorption by controlling PTHrP and RANKL expression. *Dev. Cell.* 14:674–688. doi:10.1016/j.devcel.2008.02.003

Marigo, V., R.A. Davey, Y. Zuo, J.M. Cunningham, and C.J. Tabin. 1996. Biochemical evidence that patched is the Hedgehog receptor. *Nature.* 384:176–179. doi:10.1038/384176a0

Matise, M.P., and A.L. Joyner. 1999. Gli genes in development and cancer. *Oncogene.* 18:7852–7859. doi:10.1038/sj.onc.1203243

Mullor, J.L., P. Sánchez, and A. Ruiz i Altaba. 2002. Pathways and consequences: Hedgehog signaling in human disease. *Trends Cell Biol.* 12:562–569. doi:10.1016/S0962-8924(02)02405-4

Murakami, S., and M. Noda. 2000. Expression of Indian hedgehog during fracture healing in adult rat femora. *Calcif. Tissue Int.* 66:272–276. doi:10.1007/PL00005843

Murray, D., P. Precht, R. Balakir, and W.E. Horton Jr. 2000. The transcription factor deltaEF1 is inversely expressed with type II collagen mRNA and can repress Col2a1 promoter activity in transfected chondrocytes. *J. Biol. Chem.* 275:3610–3618. doi:10.1074/jbc.275.5.3610

Nieuwenhuis, E., and C.C. Hui. 2005. Hedgehog signaling and congenital malformations. *Clin. Genet.* 67:193–208. doi:10.1111/j.1399-0004.2004.00360.x

Nishimura, G., I. Manabe, K. Tsushima, K. Fujiu, Y. Oishi, Y. Imai, K. Maemura, M. Miyagishi, Y. Higashi, H. Kondoh, and R. Nagai. 2006. DeltaEF1 mediates TGF-beta signaling in vascular smooth muscle cell differentiation. *Dev. Cell.* 11:93–104. doi:10.1016/j.devcel.2006.05.011

Ohba, S., H. Kawaguchi, F. Kugimiya, T. Ogasawara, N. Kawamura, T. Saito, T. Ikeda, K. Fujii, T. Miyajima, A. Kuramochi, et al. 2008. Patched1 haploinsufficiency increases adult bone mass and modulates Gli3 repressor activity. *Dev. Cell.* 14:689–699. doi:10.1016/j.devcel.2008.03.007

Papin, C., L.A. van Grunsven, K. Verschueren, D. Huylebroeck, and J.C. Smith. 2002. Dynamic regulation of Brachyury expression in the amphibian embryo by XSIP1. *Mech. Dev.* 111:37–46. doi:10.1016/S0925-4773(01)00599-8

Postigo, A.A., and D.C. Dean. 1997. ZEB, a vertebrate homolog of *Drosophila* Zfh-1, is a negative regulator of muscle differentiation. *EMBO J.* 16: 3935–3943. doi:10.1093/emboj/16.13.3935

Provot, S., and E. Schipani. 2005. Molecular mechanisms of endochondral bone development. *Biochem. Biophys. Res. Commun.* 328:658–665. doi:10.1016/j.bbrc.2004.11.068

Provot, S., H. Kempf, L.C. Murtaugh, U.I. Chung, D.W. Kim, J. Chyung, H.M. Kronenberg, and A.B. Lassar. 2006. Nkx3.2/Bapx1 acts as a negative regulator of chondrocyte maturation. *Development.* 133:651–662. doi:10.1242/dev.02258

Reid, L.H., R.G. Gregg, O. Smithies, and B.H. Koller. 1990. Regulatory elements in the introns of the human HPRT gene are necessary for its expression in embryonic stem cells. *Proc. Natl. Acad. Sci. USA.* 87:4299–4303. doi:10.1073/pnas.87.11.4299

Remacle, J.E., H. Kraft, W. Lerchner, G. Wuytens, C. Collart, K. Verschueren, J.C. Smith, and D. Huylebroeck. 1999. New mode of DNA binding of multi-zinc finger transcription factors: deltaEF1 family members bind with two hands to two target sites. *EMBO J.* 18:5073–5084. doi:10.1093/emboj/18.18.5073

Rodda, S.J., and A.P. McMahon. 2006. Distinct roles for Hedgehog and canonical Wnt signaling in specification, differentiation and maintenance of osteoblast progenitors. *Development.* 133:3231–3244. doi:10.1242/dev.02480

Rosen, V., J. Capparella, D. McQuaid, K. Cox, R.S. Thies, J. Song, and J. Wozney. 1993. Development of immortalized cells derived from 13DPC mouse limb buds as a system to study the effects of recombinant human bone morphogenetic protein-2 (rhBMP-2) on limb bud cell differentiation. *Prog. Clin. Biol. Res.* 383A:305–315.

Rupp, R.A., L. Snider, and H. Weintraub. 1994. Xenopus embryos regulate the nuclear localization of XMyoD. *Genes Dev.* 8:1311–1323. doi:10.1101/gad.8.11.1311

Sekido, R., K. Murai, J. Funahashi, Y. Kamachi, A. Fujisawa-Sehara, Y. Nabeshima, and H. Kondoh. 1994. The delta-crystallin enhancer-binding protein delta EF1 is a repressor of E2-box-mediated gene activation. *Mol. Cell. Biol.* 14:5692–5700.

Sekido, R., T. Takagi, M. Okanami, H. Moribe, M. Yamamura, Y. Higashi, and H. Kondoh. 1996. Organization of the gene encoding transcriptional repressor deltaEF1 and cross-species conservation of its domains. *Gene.* 173:227–232. doi:10.1016/0378-1119(96)00185-0

Sekido, R., K. Murai, Y. Kamachi, and H. Kondoh. 1997. Two mechanisms in the action of repressor deltaEF1: binding site competition with an activator and active repression. *Genes Cells.* 2:771–783. doi:10.1046/j.1365-2443.1997.1570355.x

Smith, A.N., M.L. Barth, T.L. McDowell, D.S. Moulin, H.N. Nuthall, M.A. Hollingsworth, and A. Harris. 1996. A regulatory element in intron 1 of the cystic fibrosis transmembrane conductance regulator gene. *J. Biol. Chem.* 271:9947–9954. doi:10.1074/jbc.271.17.9947

Smits, P., P. Dy, S. Mitra, and V. Lefebvre. 2004. Sox5 and Sox6 are needed to develop and maintain source, columnar, and hypertrophic chondrocytes in the cartilage growth plate. *J. Cell Biol.* 164:747–758. doi:10.1083/jcb.200312045

Später, D., T.P. Hill, R.J. O'sullivan, M. Gruber, D.A. Conner, and C. Hartmann. 2006. Wnt9a signaling is required for joint integrity and regulation of Ihh during chondrogenesis. *Development.* 133:3039–3049. doi:10.1242/dev.02471

St-Jacques, B., M. Hammerschmidt, and A.P. McMahon. 1999. Indian hedgehog signaling regulates proliferation and differentiation of chondrocytes and is essential for bone formation. *Genes Dev.* 13:2072–2086. doi:10.1101/gad.13.16.2072

Stone, D.M., M. Hynes, M. Armanini, T.A. Swanson, Q. Gu, R.L. Johnson, M.P. Scott, D. Pennica, A. Goddard, H. Phillips, et al. 1996. The tumour-suppressor gene patched encodes a candidate receptor for Sonic hedgehog. *Nature.* 384:129–134. doi:10.1038/384129a0

Takagi, T., H. Moribe, H. Kondoh, and Y. Higashi. 1998. DeltaEF1, a zinc finger and homeodomain transcription factor, is required for skeleton patterning in multiple lineages. *Development.* 125:21–31.

Tavella, S., R. Biticchi, A. Schito, E. Minina, D. Di Martino, A. Pagano, A. Vortkamp, W.A. Horton, R. Cancedda, and S. Garofalo. 2004. Targeted expression of SHH affects chondrocyte differentiation, growth plate organization, and Sox9 expression. *J. Bone Miner. Res.* 19:1678–1688. doi:10.1359/JBMR.040706

Terraz, C., D. Toman, M. Delauche, P. Ronco, and J. Rossert. 2001. delta Ef1 binds to a far upstream sequence of the mouse pro-alpha 1(I) collagen gene and represses its expression in osteoblasts. *J. Biol. Chem.* 276:37011–37019. doi:10.1074/jbc.M104185200

Tickle, C. 2004. The contribution of chicken embryology to the understanding of vertebrate limb development. *Mech. Dev.* 121:1019–1029. doi:10.1016/j.mod.2004.05.015

Tylzanowski, P., K. Verschueren, D. Huylebroeck, and F.P. Luyten. 2001. Smad-interacting protein 1 is a repressor of liver/bone/kidney alkaline phosphatase transcription in bone morphogenetic protein-induced osteogenic differentiation of C2C12 cells. *J. Biol. Chem.* 276:40001–40007. doi:10.1074/jbc.M104112200

Tylzanowski, P., D. De Valck, V. Maes, J. Peeters, and F.P. Luyten. 2003. Zfhx1a and Zfhx1b mRNAs have non-overlapping expression domains during chick and mouse midgestation limb development. *Gene Expr. Patterns.* 3:39–42. doi:10.1016/S1567-133X(02)00092-3

Verschueren, K., J.E. Remacle, C. Collart, H. Kraft, B.S. Baker, P. Tylzanowski, L. Nelles, G. Wuytens, M.T. Su, R. Bodmer, et al. 1999. SIP1, a novel zinc finger/homeodomain repressor, interacts with Smad proteins and binds to 5′-CACCT sequences in candidate target genes. *J. Biol. Chem.* 274:20489–20498. doi:10.1074/jbc.274.29.20489

Vortkamp, A., K. Lee, B. Lanske, G.V. Segre, H.M. Kronenberg, and C.J. Tabin. 1996. Regulation of rate of cartilage differentiation by Indian hedgehog and PTH-related protein. *Science.* 273:613–622. doi:10.1126/science.273.5275.613

Watanabe, Y., K. Kawakami, Y. Hirayama, and K. Nagano. 1993. Transcription factors positively and negatively regulating the Na,K-ATPase alpha 1 subunit gene. *J. Biochem.* 114:849–855.

Williams, T.M., D. Moolten, J. Burlein, J. Romano, R. Bhaerman, A. Godillot, M. Mellon, F.J. Rauscher III, and J.A. Kant. 1991. Identification of a zinc finger protein that inhibits IL-2 gene expression. *Science.* 254:1791–1794. doi:10.1126/science.1840704

Yoshida, C.A., H. Yamamoto, T. Fujita, T. Furuichi, K. Ito, K. Inoue, K. Yamana, A. Zanma, K. Takada, Y. Ito, and T. Komori. 2004. Runx2 and Runx3 are essential for chondrocyte maturation, and Runx2 regulates limb growth through induction of Indian hedgehog. *Genes Dev.* 18:952–963. doi:10.1101/gad.1174704